Available online at www.sciencedirect.com
SCIENCE DIRECT®
Journal of Nuclear Materials 337–339 (2005) 707–711
journal of nuclear materials
www.elsevier.com/locate/jnucmat

Tungsten erosion under plasma heat loads typical for ITER type I ELMs and disruptions

I.E. Garkusha [a,*], A.N. Bandura [a], O.V. Byrka [a], V.V. Chebotarev [a], I.S. Landman [b], V.A. Makhlaj [a], A.K. Marchenko [a], D.G. Solyakov [a], V.I. Tereshin [a], S.A. Trubchaninov [a], A.V. Tsarenko [a]

[a] *Institute of Plasma Physics of the NSC KIPT, 61108 Kharkov, Ukraine*
[b] *Forschungszentrum Karlsruhe, IHM, 76021 Karlsruhe, Germany*

Abstract

The behavior of pure sintered tungsten under repetitive plasma heat loads of $\sim$1 MJ/m^2 (which is relevant to ITER ELMs) and 25 MJ/m^2 (ITER disruptions) is studied with the quasi-steady-state plasma accelerator QSPA Kh-50. The ELM relevant heat loads have resulted in formation of two kinds of crack networks, with typical sizes of 10–20 μm and $\sim$1 mm, at the surface. Tungsten preheating to 600 °C indicates that fine intergranular cracks are probably caused by thermal stresses during fast resolidification of the melt, whereas large cracks are the result of ductile-to-brittle transition. For several hundreds of ELM-like exposures, causing surface melting, the melt motion does not dominate the profile of the melt spot. The disruption relevant experiments demonstrated that melt motion became the main factor of tungsten damage.
© 2004 Elsevier B.V. All rights reserved.

PACS: 52.40.Hf
Keywords: Tungsten; Surface analysis; Disruption; ELM; Erosion and deposition

1. Introduction

The major part of ITER divertor armor is foreseen to be made of tungsten plates. Armor erosion caused by disruptions and edge localized modes (ELMs) is a critical issue for a good performance of the tokamak.

For the disruptions, the heat loads to ITER divertor components are anticipated to be of order Q_{disr} = (10–100) MJ/m^2 with load duration t = 1–10 ms [1]. Such an energy range is far above of that in available tokamaks. Therefore, at present for experimental study of plasma–target interaction under the high heat loads powerful plasma accelerators are applied [2,3]. In turn, the experimental results obtained are used for validation of predictive models [4–6]. Quasi-steady-state plasma accelerators (QSPA), which are characterized by much longer duration of the plasma stream in comparison with pulsed plasma guns, are especially attractive for investigations of macroscopic erosion of tokamak armor materials, under the loads expected at ITER off-normal events.

For ELMs, extrapolation of the erosion effects obtained at the present-day tokamaks to the transient peak loads of ITER also remains uncertain [7,8]. Recent

* Corresponding author. Tel.: +38 0572 356 726.
E-mail address: garkusha@ipp.kharkov.ua (I.E. Garkusha).

0022-3115/$ - see front matter © 2004 Elsevier B.V. All rights reserved.
doi:10.1016/j.jnucmat.2004.10.008

Table 1
Parameters of QSPA Kh-50 plasma streams in different working regimes

	Disruption simulation	ELM simulation regime 1	ELM simulation regime 2
Plasma stream energy density (MJ/m^2)	25–30	0.9–1.0	1.2–1.5
Heat load on target surface (MJ/m^2)	0.65–0.7	0.45	0.7–0.75
Plasma load duration (ms)	0.2–0.25	0.25	0.25
Half-height width of load (ms)	0.1–0.14	0.1–0.12	0.17
Shape of heat load	Triangular	Triangular	Bell-shaped
Maximal plasma pressure (bar)	16–18	4.8	3.2
Average plasma density (10^{16} cm^{-3})	4–8	1.5–2.5	0.5–0.7
Plasma stream diameter (cm)	10–12	12–14	18
Impact energy of ions (keV)	$\leqslant$0.6	$\sim$0.2	$\sim$0.4

experimental observations from different machines pointed out similarities and open questions, which require further investigations are overviewed in [9]. The power loads on current tokamaks associated with the type I ELMs generally do not affect the lifetime of divertor elements. However, the ITER ELMs may lead to unacceptable lifetime [9,10]; their loads are estimated as $Q_{ELM} = (1–3)$ MJ/m^2 at $t = 0.1–1$ ms [1] and the repetition frequency of an order of 1 Hz ($\sim$400 ELMs during each ITER pulse) [7]. Special investigations on material behavior at the ELM relevant loads are thus also important. To estimate the range of tolerable loads the effects of ELMs on the lifetime of plasma facing components should be experimentally simulated for large numbers of impacts with varying energy density.

This paper presents our experimental investigations of tungsten erosion mechanisms relevant to the disruptions and the type I ELMs anticipated in ITER.

2. Experimental setup

Experiments were carried out with the quasi-steady-state plasma accelerator QSPA Kh-50 [2,11]. The samples of pure sintered tungsten of EU trademark with the sizes of $50 \times 50 \times 10$ mm have been multiply exposed to hydrogen plasma fluxes in the guiding magnetic field of 0.54 T. The target irradiation scheme is described in detail in [2]. The diameter of the plasma stream exceeds the target size. Therefore, to form a necessary impact on the target surface, special diaphragms were used. After a definite numbers of exposures, the patterns of target erosion were analyzed. Surface analysis was performed with the use of profilometry, optical microscopy, microhardness, roughness and weight loss measurements. For monitoring the specified surface regions after different numbers of exposures and for melt thickness measurements, special micromarkers (of 4–10 μm in size) were inserted into these regions with a diamond pyramid used in microhardness tests.

To achieve the working regimes for simulation of both the disruptive and ELM-like plasma impacts, the plasma stream parameters were varied over a wide range by changing the dynamics and quantity of gas filling the accelerator channel and changing the voltage of the capacitor battery. Calorimetry (both in the plasma stream and at the target surface), probes and piezo-detectors as well as spectroscopic measurements were applied to determine the plasma parameters in different regimes of operation [11]. Plasma parameters for regimes chosen for simulation of disruption and type I ELM heat loads are summarized in Table 1.

In the disruption simulation regime, the plasma pressure was increased to approach the melt velocities to those calculated for ITER disruption with plasma shield pressure of 2–7 bar [4] but with essentially longer duration. A strong vapor shielding effect in disruption simulation regime is also measured. Due to the shielding only a few percent of plasma energy reached the surface.

In the ELM simulation regimes, in spite of the decreased power levels, some shielding is also registered. Even in the regime without surface melting the target heat load is about half of the impact plasma energy. The shielding in this case appears probably due to the shock wave formation under the plasma stream interaction with target surface. The layer of stopped plasma being confined by magnetic field becomes not completely transparent for the impacting plasma.

3. Experimental results

3.1. ELM relevant plasma exposures

In these experiments the melting threshold of tungsten target has been studied. Exposures of the perpendicular target to 270 pulses in the ELM simulation regime 1 (see Table 1) at the heat loads below the melting threshold showed that the surface roughness is caused by cracks in the material. First plasma pulses primarily form a network of the cracks with cell size of $\sim$1 mm. The microhardness measurements showed that cracking causes a decrease of the surface hardness. After a large number of exposures the enlargement of the cracks

and their penetration in depth is observed. The crack network is stable, which enables its use as a reference frame for microscopic analysis. Fig. 1 demonstrates that the distances between the roughness peaks correspond to network size. The shift of the whole roughness profile relatively to the reference line and protrusion of fracture edges indicates swelling of the surface layer. The growing cracks, which are developed in parallel to the surface, were found in the bulk material by cross-section analysis.

Microscopic observations showed that some small material pieces (of 12–20 μm in size) appear inside the crack meshes due to bifurcations of large cracks. The subsequent separation of such pieces from the bulk does not result in their ejection, but it immediately leads to the piece melting because of decreased heat conduction. This effect was also clearly seen for the spikes at the crack edges in spite of other surface not being melted.

The melting threshold for the regime with triangular temporal shape of the heat load was experimentally determined as ~0.55–0.57 MJ/m^2. However it decreases after a large number of exposures: the fixed target load of 0.45 MJ/m^2 became sufficient for melting onset after 150 exposures that did not initially cause melting. Probably this effect is due to parallel cracks which decrease heat transport to the bulk. Microscopic measurements showed that the thickness of appeared melt is about 1 μm.

After an initial 10 pulses the mass loss was ~0.2 mg/cm^2. Afterwards the erosion rate decreases and becomes rather constant. The increased initial loss is due to material outgassing and removal of weakly bounded fragments from the surface. Therefore, the mass loss rate is calculated for the period of stable erosion process, i.e. with exception of initial loss. After the next 250 exposures, the mass loss is ~0.4 mg/cm^2, which corresponds to the erosion rate of 1.2 nm/pulse, or 6×10^{15} at/cm^2 per pulse. Probably the erosion is due to sputtering. For applied dose of $\sim4\times10^{19}$ ion/cm^2 the sputtering yield is of 1.5×10^{-4} at/ion.

Another target was exposed to 250 pulses in the regime 2 with target heat loads above the melting threshold. A melt layer appears with the thickness of tens of μms resulting in considerably increased surface roughness in comparison with regime 1 (see Fig. 1). During the initial 100 pulses the roughness grows up to 80–100 μm and then becomes rather unchanged in magnitude. The results indicate that besides surface cracking the melting plays an important role in the roughness increase. The influence of melt motion on the surface profile becomes evident only with large number of pulses. After 250 exposures a ridge at the edge of melt spot is seen, but it still does not dominate the surface profile.

Fig. 2 shows the crumbled-off large material pieces from the regions separated by large cracks due to subsequent exposures. The size of crumbled parts achieves 400 μm. However, the sequential pulses also smooth the edges of large cracks, restrict their growth, and lead to recovering the smooth surface. Some molten edges move into the crack voids. Thus, the melt motion covers some cracks but new ones appear in places of vanished fractures.

Besides the large-size cracks, which have been registered in both regimes, fine intergranular cracks with

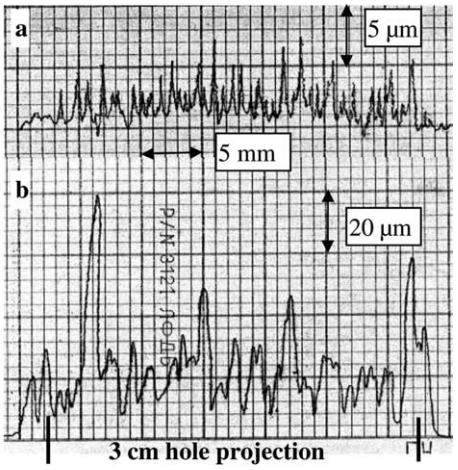

Fig. 1. Surface roughness profiles: (a) after 270 pulses in regime 1 and (b) 250 pulses in regime 2.

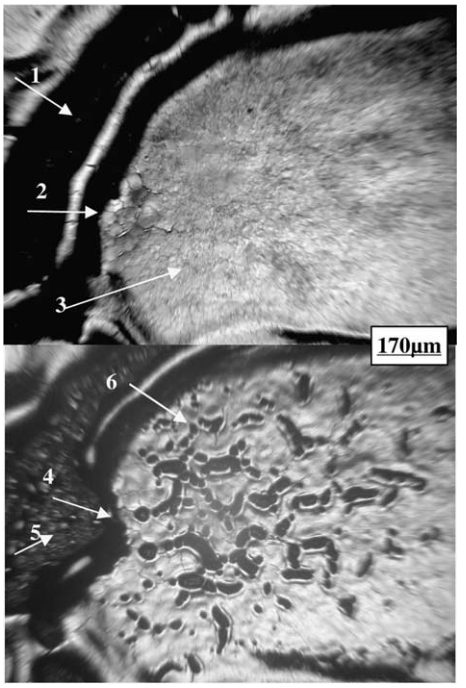

Fig. 2. Cells of crack mesh after 100 and 200 pulses in regime 2: 1– large crack, 2 – predamaged area, 3 – fine crack mesh, 4 – crumbled edge, 5 – filled crack, 6 – pits.

network of 10–30 μm were found on the resolidified surface. They appear after the melt thickness exceeds 5–10 μm. Similar fine cracks were registered in the disruption simulation experiments [2]. Thus, this is an attribute of pronounced melting only. Due to remelting, the pattern of fine cracks changes from pulse to pulse. Fine cracks become very important for the surface erosion after several hundreds pulses. Fig. 2 demonstrates considerable qualitative changes in the form of corrugation and pits that appear with increasing dosage. Such changes are accompanied by a growing mass loss rate in the regime 2. As compared to regime 1, mass loss is not constant and it increases by 2, 3 and 5 times in the course of the first 100, next 100 and next 50 pulses accordingly.

In experiments described above the target was initially at room temperature. During ITER operation the temperature of divertor targets is expected to be well above DBTT [7] and tungsten cracking can be mitigated. Therefore additional experiments on exposure of tungsten preheated at 600 °C have been started. The experimental results obtained demonstrate an absence of large cracks, while a fine crack network is still developed. Therefore, the nature of fine and large cracks looks to be completely different. Probably the fine cracks are caused by thermal stresses during fast resolidification of the melt, whereas large cracks are the result of the ductile-to-brittle transition.

3.2. Erosion of tungsten surface in disruption simulation regime

Fig. 3 presents the surface profiles after the exposures of inclined and perpendicular targets through the 2 cm diaphragm. As it is found from profilometry, the ridges of resolidified material, indicating the melt motion, arise at the melt edge. For perpendicular impacts, the height of the ridge achieve 65 μm after 20 pulses. They grows up to 130–240 μm for 75 pulses, and the distance between ridge peaks achieves 2.3–2.4 cm. The high value of the surface roughness masks the erosion crater between the ridge peaks. The melt motion is accompanied by splashing of the metal droplets of the sizes up to 100 μm onto unexposed target surface. As it was demonstrated in our previous experiments, the plasma pressure gradient is the main force initiating the melt motion [2].

For inclined exposure of the tungsten target under the angle of 20° to the surface, the formation of a mound of resolidified material is observed only at the downstream part of the melt spot. The mound height is ~35 μm, which is twice less than that found for perpendicular plasma impact. However, due to the inclination, the incoming heat flux in this case is 3 times less than for perpendicular exposure.

The cross-section of perpendicular target exposed to 75 pulses is shown in Fig. 4. Three zones are seen: a resolidified ridge of about 150 μm (top), a damaged layer with cracks down to 200 μm from the surface, and the bulk structure (bottom). Under larger magnification the structure of resolidified layer represents small equiaxial grains, which seems to be a consequence of quenching.

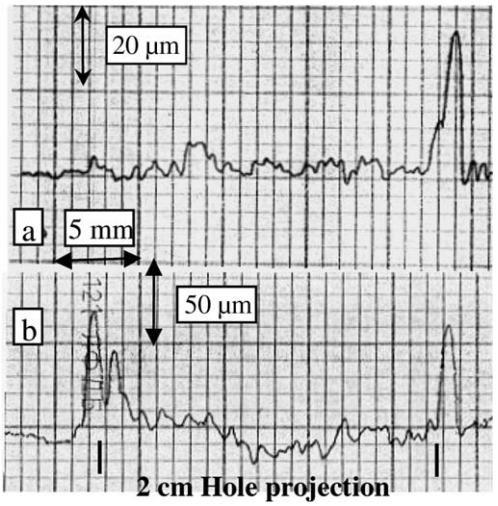

Fig. 3. Surface profiles after 20 exposures in disruption simulation regime: (a) inclined- and (b) perpendicular targets.

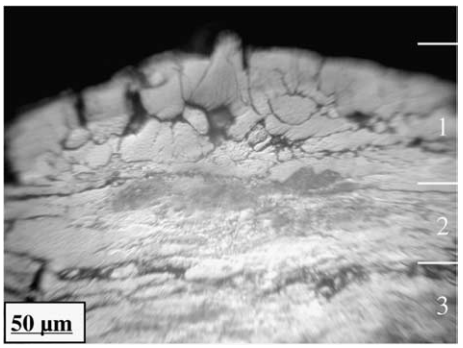

Fig. 4. Cross-section of ridge area: 1 – ridge, 2 – damaged layer, 3 – bulk.

Mass loss measurements indicated that the contribution of evaporation to the target erosion remains below 0.1 μm/pulse. For surface cracking the balance of the 2 processes is observed for increased number of exposures: the cracks become completely covered by the molten material but new thin cracks meanwhile appear.

4. Conclusions

The disruption simulation experiments showed that the melt motion driven by a plasma pressure gradient

dominates in tungsten macroscopic erosion, resulting in droplet splashing and formation of the craters with rather large edge ridges of displaced material.

The ELM relevant repetitive loads resulted in the formation of fine intergranular cracks and cracks of large sizes at the tungsten surface. For repetitive heat loads resulting in surface melting, the melt motion is detected with microscopy, but due to a low melt velocity it does not affect the profile of the melt spot until after several hundreds of pulses. The analysis of tungsten behavior for plasma loads below and above the melting threshold shows that fine intergranular cracks appear only under exposures resulted in pronounced melting.

The first results of experiments on irradiation of tungsten preheated to 600 °C indicate that fine intergranular cracks are probably caused by thermal stresses during fast resolidification of the melt, whereas large cracks are the result of ductile-to-brittle transition effects.

Fine cracks trigger a growing mass loss rate and a qualitative evolution of the sample surface starting after a few hundreds of pulses. Thus the number of ELM-like heat pulses applied in these experiments is still not sufficient either for melt motion monitoring or for reasonable prediction of material erosion in ITER. More exposures and further variations of plasma stream energies have to be performed in order to demonstrate the final damage and to estimate tolerable parameters of ITER ELMs.

Acknowledgments

This work has been performed within the WTZ project UKR-02-009 and grant M/306-2003 of Ministry of Education and Science of Ukraine.

References

[1] G. Federici et al., Nucl. Fus. 41 (2001) 1967.
[2] V.I. Tereshin et al., J. Nucl. Mater. 313–316 (2003) 686.
[3] N.I. Arkhipov et al., Fus. Eng. Des. 49&50 (2000) 151.
[4] H. Wuerz et al., J. Nucl. Mater. 307–311 (2002) 60.
[5] I. Landman et al., these Proceedings. doi:10.1016/j.jnucmat.2004.10.083.
[6] B. Bazylev et al., these Proceedings. doi:10.1016/j.jnucmat.2004.10.070.
[7] G. Federici et al., Plasma Phys. Control. Fus. 45 (2003) 1523.
[8] A. Loarte et al., Plasma Phys. Control. Fus. 45 (2003) 1549.
[9] T. Eich et al., these Proceedings. doi:10.1016/j.jnucmat.2004.10.051.
[10] G. Janeschitz et al., J. Nucl. Mater. 290–293 (2001) 1.
[11] V.V. Chebotarev et al., J. Nucl. Mater. 233–237 (1996) 736.